Processing of Titanium Foams**

By *David C. Dunand**

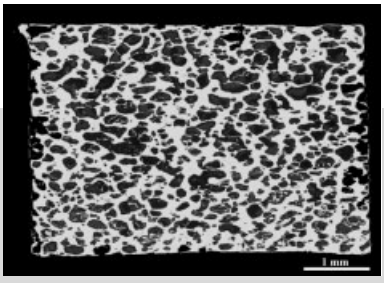

Because of their excellent mechanical properties, low density and biocompatibility, titanium foams are attractive for structural and biomedical applications. This paper reviews current techniques for titanium foam processing, which are all based on powder-metallurgy because of the extreme reactivity of liquid titanium. A first group of processes is based on powder sintering with or without place-holder or scaffolds. A second group relies on expansion of pressurized pores created during prior powder densification.

1. Introduction

The vast majority of research on the processing and synthesis of metallic foams (this term is used here interchangeably for cellular and highly-porous metals) has focused to date on melt-processing of aluminum foams with open or closed cells, as previously reviewed.[1–5] This is because the low melting point (662 °C) and low reactivity of molten aluminium make liquid-state processing relatively simple. Magnesium, with an even lower melting point (650 °C), is however more difficult to process in the liquid state into foams, due to its pyrophoric nature in air. The third technically-relevant light-metal is titanium, which exhibits excellent mechanical properties, but is much more difficult to process in the liquid state, due to its very high melting point (1670 °C). Another problem is the extreme chemical affinity of titanium with atmospheric gases (i.e., oxygen and nitrogen), which dissolve rapidly in liquid or solid titanium above ca. 400 °C, with attendant loss of ductility. Liquid titanium is also highly reactive with respect to most mold materials, thus further increasing the difficulty of melt processing. Casting of bulk titanium objects requires high-vacuum, high-temperature processing equipment. Powder metallurgy, on the other hand, can produce bulk titanium objects at much lower temperatures and under less stringent chemical reactivity constraints. Fabrication processes for titanium foams have thus to date focussed on the powder-metallurgy route and avoided the liquid route,[6] which is particularly prone to contamination because of the high surface area of foams. However, if a viable melt process could be devised for titanium foams, their cost would likely drop substantially.

Titanium-based foams have many potential applications due to titanium's outstanding mechanical properties, low density and high chemical resistance.[7] The first area of use for titanium foams is for structural applications, e.g., as sandwich core for aerospace or submarine vehicles, taking advantage of the excellent density-compensated strength and stiffness of titanium as well as its outstanding resistance to corrosion. Titanium's high melting point also allows for the use of titanium foams at elevated temperatures (e.g., for sandwich core or as heat exchanger and catalyst substrate), limited to ca. 400 °C due to the low oxidation resistance of titanium. The second area of application is for porous bone-replacement implants, where the excellent biocompatibility and mechanical properties (in particular fatigue resistance) of titanium are essential.[8–12] Also relevant for that application is the low stiffness of titanium foams, desirable to reduce the amount of stress-shielding of the bone into which the foam is implanted; stress-shielding is known to lead to bone resorption and eventual loosening of the implant.[9,13]

The present article provides a review of existing methods for the solid-state fabrication of titanium foams, which are schematically depicted in Figure 1. We do not include titanium-based intermetallic foams, and in particular NiTi foams with shape-memory or superelastic properties.[14–16]

[*] *Prof. David C. Dunand*
Department of Materials Science and Engineering,
Northwestern University,
Evanston IL 60208, USA.
E-mail: dunand@northwestern.edu

[**] *The author acknowledges the support of the US National Science Foundation (grant DMR-0108342/001) and the students involved with titanium foam research in his group: N.G.D. Murray (formerly known as N.G. Davis), S.M. Oppenheimer, C.A. Schuh and J. Teisen.*

 DOI: 10.1002/adem.200405576

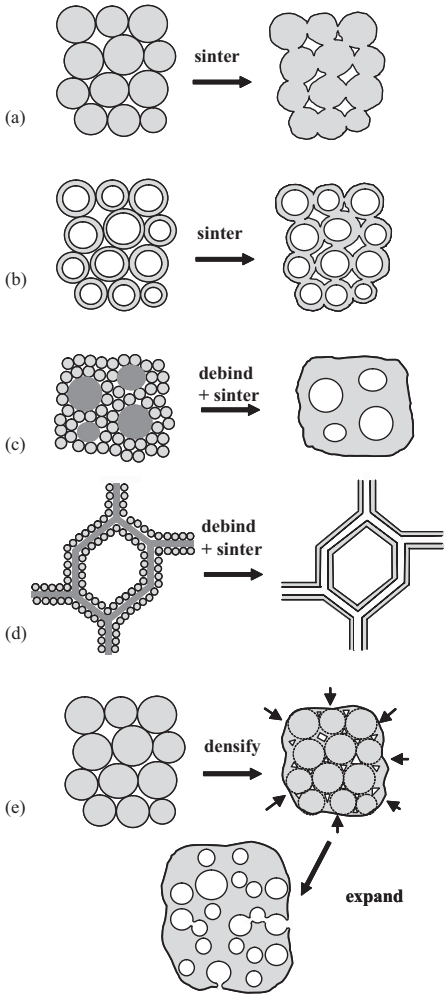

Fig. 1. Schematics of main solid-state processes used to fabricate titanium foams – (a) powder sintering – (b) hollow powder sintering – (c) formation of secondary pores by gas expansion or addition of a fugitive solid-space holder, followed by sintering – (d) sintering of powders deposited on fugitive scaffold – (e) powder densification in presence of gas, and subsequent expansion of trapped gas bubbles.

2. Processes Based on Powder Sintering

The inherent simplicity of sintering processes allows for relatively rapid, single- or two-step methods requiring little more than a high-vacuum furnace.

2.1. Sintering of Uniform Powder Preforms

The simplest technique for making a titanium foam is based on the partial sintering of a porous preform of titanium powders (Fig. 1a). Cirincione et al.[17] sintered loose Ti-6Al-4V powders at 1000 °C for times between 0.5 and 24 h., achieving porosities between 41 and 55 %. The strength was dictated by the necks formed between the powder particles, and a maximum compressive strength of 55 MPa was found for a foam with 49 % porosity. Kinetics of densification of unalloyed titanium can be accelerated by uniaxial pressing, which was investigated below and above the allotropic temperature of titanium (882 °C), resulting in porosity between 5 and 35 %.[18,19] Oh et al.[20,21] sintered spherical unalloyed titanium powders with and without applied pressure and achieved 5–37 % porosity. Young's modulus and compressive yield strength decreased linearly with increasing porosity, and at 30 % porosity, the stiffness of the porous titanium was close to that of human bone (ca. 20 GPa). The same authors[22] expanded this approach to samples with a gradient in porosity, achieved by using distinct layers of titanium powders with different particle sizes, which were co-sintered with and without applied stress. A gradient in porosity and pore size is achieved by the more rapid sintering of finest powders. Ricceri and Matteazzi[23] used a combination of cold isostatic pressing and sintering of milled Ti-6Al-4V powder to produce foams with 26 % porosity; subsequent containerless hot-isostatic pressing eliminated the closed porosity without affecting the open pores. Another way to decrease sintering time is to use spark plasma sintering[24]: CP-Ti and Ti-6Al-4V powders were consolidated to a porosity of ca. 30 % by this methods which allows much lower temperature (560–700 °C) and sintering times (3–20 min.) at relatively high pressures (20–30 MPa). A subsequent anneal at 1000 °C further improved the mechanical properties of the foams.

Thieme et al.[25] reported porosities between 35 and 60 % for sintered titanium powders, the highest value being achieved with agglomerated powders, and they measured bending strengths (ranging from 5 to 190 MPa) and Young moduli (5–80 GPa) for a large number of samples. Furthermore, they demonstrated that the sintering of coarse powder could be accelerated by adding 1.5 wt.% silicon to the titanium powders which produced a transient liquid phase, with no measurable decrease in foam strength after processing. Fi-

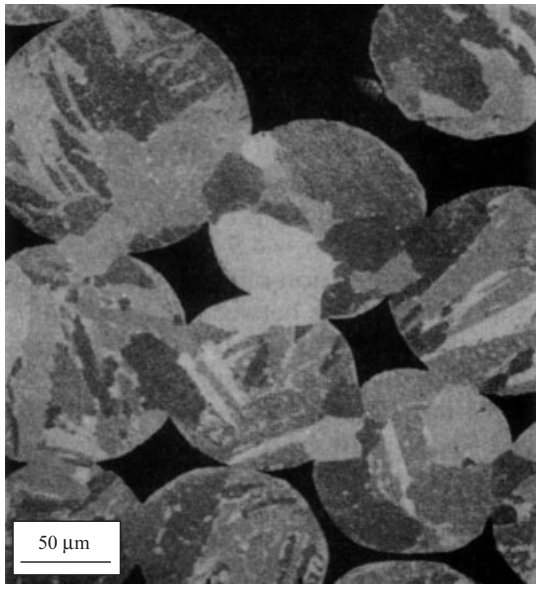

Fig. 2. Cross-section of foam produced by partial sintering of CP-Ti powders, showing sharply cusped, open porosity (porosity: 24 %) [18].

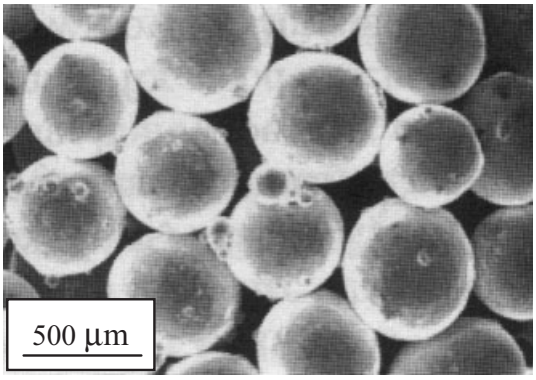

Fig. 3. SEM image of foam produced by partial sintering of hollow Ti-6Al-4V spheres (total porosity: 73 %) [28].

nally, Thieme et al.[25] produced graded titanium foams by sintering a stack of three powder layers with different particle size and silicon content. The volume fraction and pore size varied from 22 % and 48 μm for the finer powder layer, to 45 % and 200 μm for the coarser powder layer. A gradient in elastic property was also measured by scanning acoustic microscopy.

The limitation of the powder sintering approach is that pores size and shape are dictated by the titanium powder size and shape. For spherical powders, the porosity is limited to at most 50 %, and the shape of the pores is highly non-spherical. Pores are cusped at the sintering necks between powders (Fig. 2), where cracks are likely to initiate under fatigue conditions. For instance, a fatigue limit of 40 MPa for 10^6 compressive cycles was found by Asaoka et al.[26] for a sintered Ti foam with 42 % porosity, much less that the static compressive strength of 182 MPa.

A solution to the problem of low pore fraction produced during sintering of titanium powders is to use titanium wires: this was demonstrated with a 130 μm diameter crimpled wire sintered near 1600 °C, resulting in a open-cell foam with 45–50 % porosity (this value could be easily increased by reducing the sintering temperature).[27] Another approach is to sinter hollow powders (Fig. 1b): porosity then consists of the inner space of the porous powders as well as the space between the powders due to partial sintering. This approach was demonstrated by Sypeck *et al.*,[28] who produced a foam with 73 % porosity by sintering 0.5–1.4 mm diameter hollow Ti-6Al-4V spheres (a by-product of gas atomisation) for 24 h. at 1000 °C (Fig. 3). Only a weak bonding was observed between the spheres due to their large size, resulting in relatively low compressive strength (6.2 MPa).

2.2. Sintering of Non-Uniform Powder Preforms Made with a Gaseous Blowing Agent

In this approach, large, secondary pores are created by a gas within a preform consisting of titanium powders and small, primary pores; upon sintering, the primary pores are eliminated rapidly, while the much larger secondary pores remain unchanged (Fig. 1c). The advantage of this method is that the shape and volume fraction of the secondary pore can be controlled independently of the titanium powder characteristics. The disadvantages are the large size of the secondary pores as compared to the titanium powders, contamination from the binder used together with the titanium powders, and residual primary porosity due to incomplete sintering. Also, uniaxial pressing cannot be used to improve sintering, as it would produce collapse of the secondary pores.

Jee et al.[29] used a CO_2-based blowing agent to create large secondary pores within a mixture of titanium powders, binder and surfactant. After foaming and air pyrolysis, reticulated metallic foams with 90–95 % porosity and cell size of ca. 0.4 mm were formed. Subsequent sintering of the titanium struts was only partially successful, because of ash residues (3–4 wt.%) from the resin pyrolysis. This technique was also applied to Ti-15V-3Cr-3Al-3Sn (wt.%).[30]

In an approach combining the above gas-blowing process with the hollow-sphere process, Hurysz et al.[31] produced hollow titanium spheres by injecting a slurry of titanium hydride and polymer binder in a solvent through a co-axial nozzle. Thermal treatment in an inert atmosphere removed the binder within the green bubbles, decomposed the hydride and sintered the titanium powders in the sphere walls to a density over 96 %, resulting in titanium spheres with 1–6 mm diameter and 0.1 mm wall thickness. If sintered together, these spheres would result in a foam with ca. 86 % porosity.

2.3. Sintering of Non-Uniform Powder Preforms Containing a Solid Space Holder

Another approach to make large secondary pores within a titanium powder preform is to use a "space holder", consisting of a solid material which can be removed, usually at low temperature, without excessive contamination of the titanium powders. The mixture of metallic powders and space-holder powders can then be pressed, thus imparting enough green strength to the metal powder to prevent collapse upon removal of the space-holder and subsequent sintering (Fig. 1c).

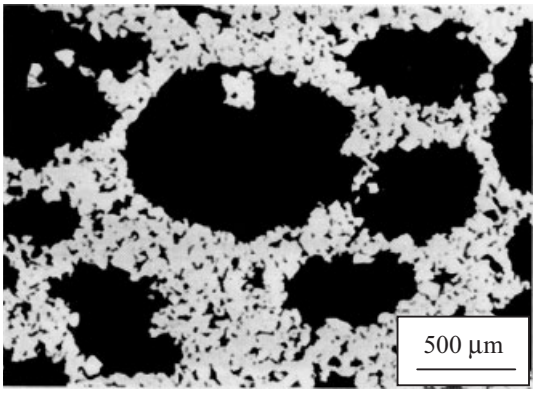

Fig. 4. Cross-section of titanium foam produced by sintering of powders after removal of a fugitive place holder (porosity: 67 %) [38].

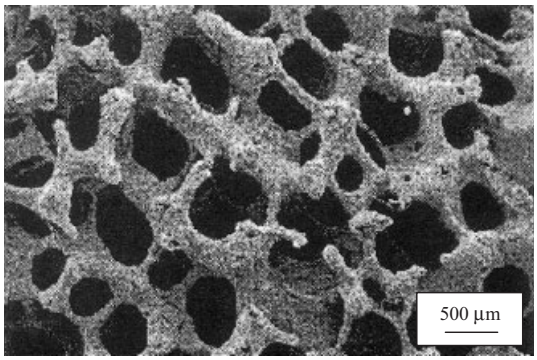

Fig. 5. SEM micrograph of reticulated Ti-6Al-4V foam produced by sintering of powders deposited onto a fugitive scaffold (porosity:> 80 %) [42].

In an early article, Wheeler et al.[32] used magnesium powders as space holder, which were removed by evaporation at 1000 °C, followed by sintering at 1400 °C of the Ti or Ti-6Al-4V powders into the foam structure. Elongated pores were achieved by using Mg wires (0.18–0.45 mm in diameter). Foams exhibited 25–82 % porosity, strengths of 15–607 MPa, and Young's moduli of 3–9 GPa. Kostornov et al.[33,34] sintered a blend of Ti with up to 7 wt.% Cu and 5–30 % stearin. The combination of wax space holder and metallic alloying addition producing a transient liquid phase resulted in foams with 25–70 % porosity, for which the authors reported tensile, shear and bending strengths as well as impact toughness.

Bram et al.[35] used carbamide (urea) powders which were removed below 200 °C, with minimal contamination of the titanium powders. Subsequent sintering at 1400 °C for 1 h resulted in foams with porosity in the range 60–77 % and pore size in the range 0.1–2.4 mm, controlled by the carbamide particle size. The authors reported compressive and bending mechanical properties for these foams, e.g. a plateau stress of ca. 10 and 100 MPa for porosities of 77 and 60 %, respectively. Wen et al.[36] used ammonium hydrogen carbonate as space holder, with decomposition at 200 °C and titanium sintering at 1200 °C for 2 h. The resulting foam with a porosity of 78 % exhibited a compressive strength of 35 MPa and a Young's modulus of 5.3 GPa. These values were a close match to those for cancellous bone, 3–20 MPa and 10–40 GPa, respectively. No information was provided for the contamination levels of the titanium. Later, these authors produced by the same method foams with 35–80 % porosity with a wide range of strength and stiffness showing a good match to both human cancellous and cortical bone.[11,37] They also reported the growth of a bonelike apatite layer throughout the foam.[37] Rausch and Banhart [38] used polymer granules as space holder, which were removed chemically at 130 °C. Sintering at 1100–1250 °C produced foams with 55–80 % porosity (Fig. 4) with a tensile strength range of 1.5–30 MPa, and Young's modulus of 0.3–16 GPa. The authors noted that microporosity within the sintered network decreased strength and could be reduced by partial addition of titanium hydride.

Tuchinskiy and Loutfy[39] recently described an interesting variation on the above method. First, they extruded rods consisting of a fugitive core and a shell made of titanium powder and polymer binder. The rods were cut into segments which were poured into a die and compressed into a green body. The core material and binder were then removed at low temperature and the powder vacuum-sintered at 1200–1300 °C, resulting in a titanium foam containing elongated secondary pores. The authors suggest that honeycomb structures could be produced by aligning the rod segments before pressing.

Andersen et al.[40] used the space-holder technique to produce hollow spheres, by coating Styrofoam spheres with titanium powders and a binder suspension in a fluidised bed. The polymer was then removed by heat-treatment, and the green spheres were sintered, resulting in hollow titanium spheres, with 4 mm diameter and 0.125 mm wall thickness. Subsequent sintering of these spheres would lead to very low density foams, but was not attempted, presumably due to contamination of the titanium during processing.

2.4. Sintering of Powders Deposited on a Fugitive Scaffold

An approach, which is related to the above technique using a fugitive space holder, uses a polymer scaffold which is repeatedly coated with a mixture of titanium powders and binder. After removal of the scaffold and binder, and subsequent sintering of the powders, a reticulated open-cell foam with hollow titanium struts results (Fig. 1d), as demonstrated recently by Kupp et al.[41] Three types of pore are present in these foams, which are in order of increasing size: primary porosity within the struts (if sintering was incomplete), secondary porosity at the core of the struts (previously occupied by the scaffold), and open tertiary porosity between struts. Li et al.[42] used this process with Ti-6Al-4V powders and polyurethane elastomeric scaffold foams and fabricated reticulated foams with 88 % porosity and compressive strength of 10 MPa (Fig. 5). They later showed that a second deposition of powders slurry on a previously-sintered foam followed by

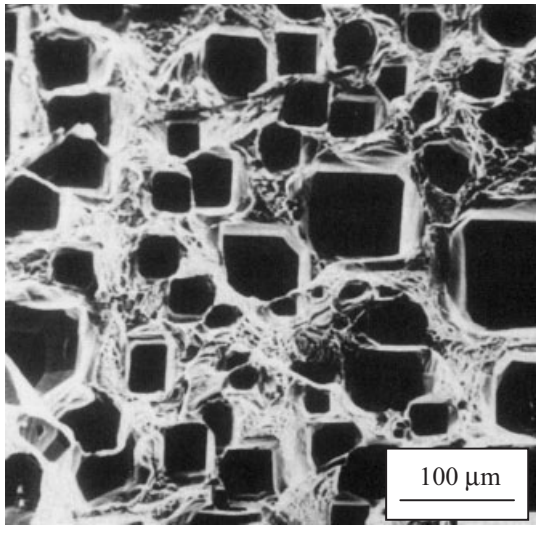

Fig. 6. SEM micrograph of tensile fracture surface of Ti-6Al-4 V foam, produced by densification of powders in the presence of argon, and subsequent creep expansion of the entrapped argon pores (porosity: > 25 %) [45].

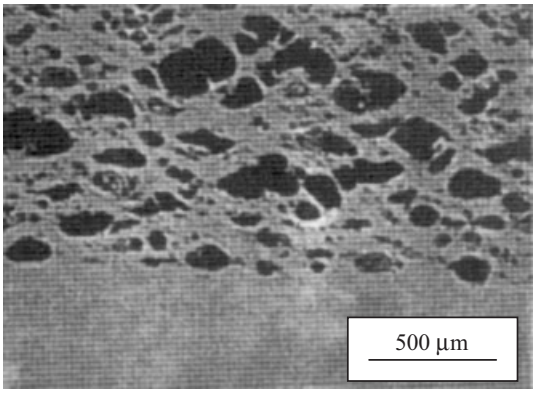

Fig. 7. Cross-section of Low-Density-Core Ti-6Al-4V sheet, consisting of a dense face sheet and a porous core produced by creep expansion of entrapped argon pores (core porosity: 40 %) [50].

a second sintering resulted in increased density and much improved compressive strength (80 % and 36 MPa, respectively), as a result of healing of flaws in the titanium struts.[43]

3. Processes Based on Expansion of Pressurized Bubbles

The sintering processes described in the previous section all have in common that the shape, size and volume fraction of the pores in the final titanium foam are dictated by those of the original (primary and secondary) pores in the powder preform. Furthermore, sintering processes do not allow easy control of the level of pore connectivity to each other and the surface. By contrast, the creep and superplastic expansion processes described in the present section result in titanium foams exhibiting pores with shape, size, connectivity and volume fraction independent of those in the original powder preform. The process route is however more complicated, as it requires high-pressure and -temperature equipment, and necessitates two separate heat-treatment steps (the first for powder compaction and the second for bubble expansion). Also, pore volume fractions rarely exceed 50 %.

3.1. Creep Expansion Processes

3.1.1. Argon Expansion Process

Foaming by solid-state expansion of pressurized pores was first described by Kearns et al.[44,45] for Ti-6Al-4V foams, and is schematically depicted in Figure 1e. In a first step, powders are packed into a steel canister which is evacuated and backfilled with argon gas. Then, the powders are densified by Hot Isostatic Pressing (HIP), and, because argon is neither soluble nor reactive with titanium, the gas is entrapped within a continuous titanium matrix in the form of isolated, micron-sized, high-pressure argon bubbles with a low volume fraction (typically less than 1 %). Finally, after cooling and removal of the steel canister, the titanium billet is exposed to elevated temperatures at ambient pressure (or under vacuum). The reduced strength of the titanium matrix at elevated temperature allows the expansion of the high-pressure gas bubbles, in a process similar to foaming of viscous polymer melt containing pressurized gas bubbles.

Kearns et al.[44,45] found that increasing the argon backfill pressure or the foaming temperature increased the foam porosity, as a result of the reduction in creep strength of the matrix. At the highest temperature of 1240 °C and with 0.1 atm backfill pressure, the pore growth kinetics was found to monotonically decrease with time, with ultimate porosity of ca. 30 % reached after ca. 12 h (porosity as high as 40 % are reported, but with no information on experimental conditions). This effect is due to the decrease in gas pressure in the pores, associated with the increase in pore diameter. Above 1000 °C, the pores adopted a cubic, facetted morphology, as a result of surface diffusion and anisotropic surface energies (Fig. 6). Additionally, Kearns et al.[44,45] showed that the argon-filled pores could be elongated by hot-working of the billets, resulting in a highly anisotropic expansion upon subsequent foaming.

Later, Dunand et al.[46,47] demonstrated the Kearns process for commercial-purity titanium (CP-Ti). They investigated lower temperatures (903 and 960 °C) and achieved porosity of 26 % in times as short as 30 min., as a result of the reduced creep strength of CP-Ti as compared to Ti-6Al-4V and of the increased backfill pressure (3.3 atm.). For foams with 22 % porosity, a yield stress of 200 MPa and a Young's modulus of 60 GPa were measured.

Recently, Ricceri and Matteazzi[48] used a variation of the Kearns process, by replacing argon with hydrogen produced *in-situ* by hydride decomposition. The authors cold-compacted titanium powders in which 5 or 10 wt.% TiH_2 powders had been blended. These blends were then HIP-consolidated into a partially porous billet where complete decomposition of the TiH_2 was avoided by the high pressure. After removing the can, the samples were reheated in the HIP to the foaming

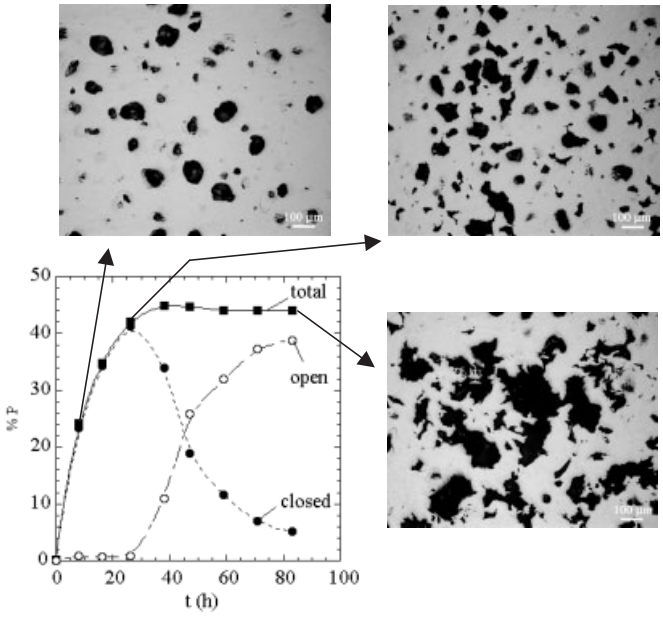

Fig. 8. Total, open and closed porosity vs. time and pore morphology evolution during superplastic foaming of CP-Ti [62].

temperature (950–1150 °C) under isostatic pressure. Upon pressure release, internally-pressurized hydrogen bubbles are formed by decomposition of TiH_2. These bubbles grew by creep deformation of the matrix, resulting in foams with porosities in the range 17–24 % after one hour of foaming. As compared to the Kearns argon process, a much larger amount of gas can be incorporated in the billet; however, unlike argon, hydrogen has very high solubility and diffusivity in titanium, rapidly reducing the pressure in the bubbles and the driving force for foaming.

3.1.2. Low-Density Core Process

Martin and Lederich[49] adapted the Kearns argon expansion process to the integral fabrication of sandwich structures. They used Ti-6Al-4V flat canisters (rather than steel canisters), which were filled with low-cost blended elemental particles of CP-Ti and 60Al-40V (rather than pre-alloyed Ti-6Al-4V gas-atomized powders). Foaming occurs without removal of the canister, which becomes the face-sheets of a sandwich structure. They called their process the Low-Density Core (LDC) process, and reported porosities of 25 % in the foamed core. They also indicated that forging, extrusion and shape-milling could convert HIP billets to smaller sections. In a later publication,[50] large sheets (2 m x 1.2 m x 4 mm) with ca. 40 % porosity core porosity were reported (Fig. 7). Deformation of the sheet by hot rolling, forging, die forming or drape forming before or after the core expansion was also demonstrated.

Elzey and Wadley[51] subsequently modelled the open-die forging of LDC sandwiches, and predicted that densification occurs first in the centre of the work-piece, and propagates as a front toward the outer edges, resulting in a complex non-uniform densification behavior. Queheillalt et al.[52] performed an experimental study of foaming of rolled Ti-6Al-4V LDC precursors. They used eddy-current and laser ultrasonic sensors to determine the evolution of relative density and elastic moduli *in-situ* during heat treatment. Core porosity increased during initial heating and stabilized to ca. 27% after an additional anneal for 4.5 h at 920 °C. The resulting sandwich (core and face sheets) exhibited a Young's modulus of 45 GPa. Initial pores were highly elongated due to rolling and became more equiaxed after foaming. Vancheeswaran et al.[53] developed a microstructure-dependent model based on a representative volume element consisting of a single pressurized spheroidal pore expanding within a matrix deforming by dislocation creep or grain-boundary sliding.

Elzey and Wadley[54] later published an analysis of the time dependence of porosity, in terms of pore size and spacing and process conditions. They first use an existing model based on expansion of a pressure vessel deforming by power-law creep to describe the early stage of foaming. They then consider void coalescence based on a percolation threshold approach. Their model predicts that the maximum achievable porosity for the core of a LDC material is less than 50 %. They point out that this upper limit under superplastic condition could increase to 65 %, which is however much lower than the values achievable by semi-solid and liquid state processes.

3.2. Superplastic Expansion Processes

The foaming processes described in the previous section (3.1) exhibit slow kinetics due to the low deformation rates displayed by titanium under creeping conditions. Also, foaming under creeping conditions allows only for modest porosities, because walls between adjacent pores fracture at relatively small strain. This allows for the merging of pores with each other and with the billet surface, which leads to the escape of the foaming gas. A possible solution to these limitations is to induce superplasticity in the titanium matrix during foaming: as compared to creep, superplastic deformation is characterized by faster deformation rates (i.e., faster foaming rates) and higher tensile ductility (i.e., higher terminal porosities). Dunand and Teisen[46] first demonstrated that superplasticity could be used for solid-state foaming of CP-Ti and Ti-6Al-4V. They used transformation superplasticity, which is activated by thermal cycling around the allotropic transformation of CP-Ti[55,56] and Ti-6Al-4V,[57–59] rather than fine-grain superplasticity, which is difficult to achieve in CP-Ti (due to grain growth) or in Ti-6Al-4V (unless a complex thermo-mechanical treatment is given).

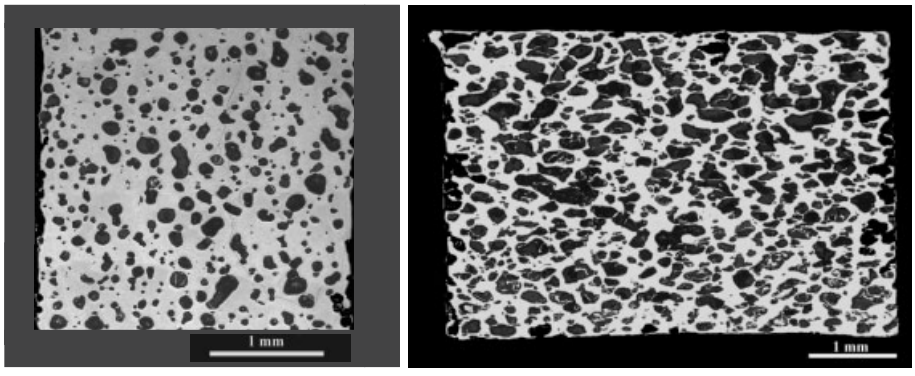

Fig. 9. Micrographs of CP-Ti foams produced by expansion of Ar pores with a superimposed uniaxial 1 MPa stress (stress axis is horizontal). (a) foamed under creep conditions at 903 °C for 11.8 h. (porosity: 20 %) (b): foamed under superplastic conditions by cycling between 830 and 980 °C for 11.8 h. (porosity: 41 %) [47].

Davis et al.[47] demonstrated that the overall foaming rate of CP-Ti is significantly higher under cyclic superplastic conditions (830–980 °C) than under isothermal creep conditions at the corresponding effective temperature (903 °C). Furthermore, the terminal porosity is also much higher for the superplastically-foamed specimens. Even when the cycling experiments are compared to isothermal creep experiments at 960 °C (well above the effective temperature and near the maximum cycling temperature of 980 °C), terminal

total porosities are larger for the cycled specimens. Confirmation of the beneficial effect of superplastic foaming was given in a further study where the temperature cycling frequency and range were systematically changed.[60] Modelling of the pore expansion within a creeping titanium matrix was performed by continuum mechanics and by the finite-element method, which allowed the study of pore clustering and pore size distribution.[61]

Another study[62] focussed on the evolution of pore microstructure for specimens superplastically foamed under thermal cycling conditions. As shown in Figure 8, foaming for 8 h. resulted in rapid growth of pores (from 2–3 to 100 μm) which are mostly rounded and generally equiaxed. During the following 18 h of thermal cycling, pore size increased at a lesser rate and internal pore coalescence occurred. The fact that porosity stopped to increase before significant opening of the pores to the surface (and escape of the gas) indicated that the gas pressure was too low to affect further pore expansion. However, in the following 57 h, the mostly equiaxed pores became very jagged and achieve much larger pore dimensions (up to 500 μm). This was due to extensive pore coalescence through rupture of the very thin walls made possible by the high ductility achievable during superplastic deformation. The fractured thin walls became protrusions within the coalesced pores, giving them a jagged morphology. Similar results were obtained recently by Li et al.,[63] where porosities as high as 53 % were achieved for CP-Ti under thermal cycling conditions. The authors also carried out a finite-element study of the mechanical properties of the foams with and without bone ingrowth within the pores.

Davis et al.[47] performed experiments where titanium foaming took place with a superimposed uniaxial stress under either superplastic or creep conditions. While the total porosity was not affected by the applied stress, the pores in the superplastic foams were notably elongated in the direction of the applied stress, with an aspect ratio as high as 5 and a length of up to 1 mm (Fig. 9). The yield stress and Young's modulus for a superplastic foam with 41 % porosity was about 120 MPa and 39 GPa. Murray et al.[64] also studied the case where the phase transformation of titanium was induced by chemical cycling through cyclic alloying and de-alloying with hydrogen, rather than thermal cycling. Foaming by chemical cycling was slower than by thermal cycling because of the lower cycling frequency achievable. However, similar foaming kinetics were observed when foaming was considered on a per-cycle basis. Additionally, similar terminal porosities were found for either chemical or thermal cycling foaming.

4. Summary

Titanium foams are attractive for structural and biomedical applications. Unlike aluminum foams, they cannot easily be produced in the liquid state, due to the high melting temperature and extreme contamination susceptibility of titanium. All existing processes are based on powder metallurgy and can be classified into two groups:

1. Powder sintering processes - A first approach is based on partial sintering of loose titanium powders into a porous body, with porosity in the range 20–50 % and low strength at the higher porosity. Alternatively, hollow titanium powders or spheres can be used to increase porosity. Another approach uses a gas or fugitive solid particles to create larger pores around which the titanium powders are then fully sintered as struts or walls. In a variation to this approach, powders deposited upon a fugitive scaffold are sintered into a reticulated foam. Higher porosities can be reached (up to 90 %) with a good control of pore morphology, but the pores are always open and they are much larger than the original titanium powders.

2. Pressurized pore expansion processes – First, argon gas is entrapped in titanium by hot-compaction of a powder preform. The resulting high-pressure argon bubbles are then expanded by exposure to high temperature, where the densified titanium matrix creeps rapidly. A variation on this process uses a titanium canister which is not removed before expansion, resulting in a titanium sandwich structure. An improvement of this process utilizes superplasticity in the matrix during pores expansion, allowing for faster foaming rates and higher porosity (as high as 53 %) with good strength values. In the pore expansion processes, the pore size and connectivity can be tailored.

Received: December 12, 2003

[1] M. F. Ashby, A. Evans, N. A. Fleck, L. J. Gibson, J. W. Hutchinson, H. N. G. Wadley, *Metal Foams: A Design Guide*, **2000**, Butterworth-Heinemann, Boston.
[2] J. Banhart, *JOM-J. Miner. Met. Mater. Soc.* **2000**, *52*, 22.
[3] J. Banhart, *Prog. Mater. Sci.* **2001**, *46*, 559.
[4] J. Banhart, *MRS Bull.* **2003**, *28*, 290.
[5] H. P. Degischer, B. Kriszt (Eds.), *Handbook of Cellular Metals* **2002**, Wiley, Weinheim.
[6] G. Rausch, T. Hartwig, M. Weber, O. Schulz, *Materialwiss. Werkstofftech.* **2000**, *31*, 412.
[7] M. J. Donachie, *Titanium – a Technical Guide*, **1988**, ASM, Metals Park, OH.
[8] J. L. Nilles, Karagian.Mt, K. R. Wheeler, *J. Biomed. Mater. Res.* **1974**, *8*, 319.
[9] S. J. Simske, R. A. Ayers, T. A. Bateman, *Mater. Sci. Forum* **1997**, *250*, 151.
[10] M. J. Donachie, *Adv. Mater. Proc.* **1998**, *7*, 63.
[11] C. E. Wen, Y. Yamada, K. Shimojima, Y. Chino, T. Asahina, M. Mabuchi, *J. Mater. Sci.-Mater. Med.* **2002**, *13*, 397.
[12] S. L. Thelen, F. Barthelat, L. C. Brinson, *J. Biomed. Mater. Research* **2004**, *69A*, 601.
[13] B. P. McNamara, A. Toni, D. Tayor, *Advances in Engineering Materials* **1995**, *99*, 309.
[14] Y. H. Li, L. J. Rong, Y. Y. Li, *J. Alloys Compounds* **2002**, *345*, 271.
[15] D. C. Lagoudas, E. L. Vandygriff, *J. Intelligent Mater. Systems Structures* **2002**, *13*, 837.

[16] M. Assad, A. Chernyshov, M. A. Leroux, C. H. Rivard, *Bio-Medical Materials and Engineering* **2002**, *12*, 225.
[17] R. Cirincione, R. Anderson, J. Zhou, D. Mumm, W. O. Soboyejo, in *Processing and Properties of Lightweight Cellular Metals and Structures (Eds: A. Ghosh, T. Sanders and D. Claar), TMS, Warrendale*, **2002**, 189.
[18] N. Taylor, D. C. Dunand, A. Mortensen, *Acta Metall. Mater.* **1993**, *41*, 955.
[19] C. Schuh, D. C. Dunand, *Acta Mater.* **2000**, *48*, 1639.
[20] I. H. Oh, N. Nomura, S. Hanada, *Mater. Trans.* **2002**, *43*, 443.
[21] I. H. Oh, N. Nomura, N. Masahashi, S. Hanada, *Scripta Mater.* **2003**, *49*, 1197.
[22] I. H. Oh, H. Segawa, N. Nomura, S. Hanada, *Mater. Trans.* **2003**, *44*, 657.
[23] R. Ricceri, P. Matteazzi, *Intern. J. Powder Metall.* **2001**, *37*, 61.
[24] K. Asaoka M. Kon, *Mater. Sci. Forum*, **2003**, *426*, 3079.
[25] M. Thieme, K. P. Wieters, F. Bergner, D. Scharnweber, H. Worch, J. Ndop, T. J. Kim, W. Grill, *J. Mater. Sci.-Mater. Med.* **2001**, *12*, 225.
[26] K. Asaoka, N. Kuwayama, O. Okuno, I. Miura, *J Biomedical Mater. Research* **1985**, *19*, 699.
[27] G. A. W. Murray, J. C. Semple, *J. Bone Joint Surg.-Br. Vol.* **1981**, *63*, 138.
[28] D. J. Sypeck, P. A. Parrish, H. N. G. Hayden, in *Porous and Cellular Materials for Structural Applications (Eds: D. S. Schwartz, D. S. Shih, H. N. G. Wadley, A. G. Evans), MRS, Pittsburgh*, **1998**, 205.
[29] C. S. Y. Jee, N. Ozguven, Z. X. Guo, J. R. G. Evans, *Metall. Mater. Trans. B* **2000**, *31*, 1345.
[30] Z. X. Guo, C. S. Y. Jee, N. Ozguven, J. R. G. Evans, *Mat. Sci. Technol.* **2000**, *16*, 776.
[31] K. M. Hurysz, J. L. Clark, A. R. Nagel, C. U. Hardwicke, K. J. Lee, J. K. Cochran, T. H. Sanders, in *Porous and Cellular Materials for Structural Applications (Eds: D. S. Schwartz, D. S. Shih, H. N. G. Wadley, A. G. Evans), MRS, Pittsburgh*, **1998**, 191.
[32] K. R. Wheeler, M. T. Karagianes, K. R. Sump, in *Conf. Titanium Alloys in Surgical Implants (Eds: H. A. Luckey, F. Kubli), ASTM, Philadelphia*, **1983**, 241.
[33] A. G. Kostornov, S. M. Agayan, *Sov. Powder Met. Metal Cer.* **1990**, *29*, 804.
[34] A. G. Kostornov, L. G. Galstyan, S. A. Mnatsakanyan, S. M. Agayan, *Sov. Powder Met. Metal Cer.* **1986**, *25*, 909.
[35] M. Bram, C. Stiller, H. P. Buchkremer, D. Stover, H. Baur, *Adv. Eng. Mater.* **2000**, *2*, 196.
[36] C. E. Wen, M. Mabuchi, Y. Yamada, K. Shimojima, Y. Chino, T. Asahina, *Scripta Mater.* **2001**, *45*, 1147.
[37] C. E. Wen, Y. Yamada, K. Shimojima, Y. Chino, H. Hosokawa, M. Mabuchi, *J. Mater. Res.* **2002**, *17*, 2633.
[38] G. Rausch, J. Banhart, in *Handbook of Cellular Metals (Eds: H. P. Degischer, B. Kriszt), Wiley*, **2002**, 21.
[39] L. Tuchinskiy, R. Loutfy, in *Materials and Processes for Medical Devices ASM, Metals Park* **2003**, 1.
[40] O. Andersen, U. Waag, L. Schneider, *Adv. Eng. Mater.* **2000**, *2*, 192.
[41] D. Kupp, D. Claar, K. Flemmig, U. Waag, H. Goehler, in *Processing and Properties of Lightweight Cellular Metals and Structures (Eds: A. Ghosh, T. Sanders, D. Claar), TMS, Warrendale*, **2002**, 61.
[42] J. P. Li, S. H. Li, K. de Groot, P. Layrolle, in *Key Engineering Materials* **2002**, *218–220*, 51.
[43] J .P. Li, S. H. Li, K. de Groot, P. Layrolle, in *Key Engineering Materials* **2003**, *240–242, 547*.
[44] M. W. Kearns, P. A. Blenkinsop, A. C. Barber, T. W. Farthing, *Metals Mater.* **1987**, *3*, 85.
[45] M. W. Kearns, P. A. Blenkinsop, A. C. Barber, T. W. Farthing, *Intern. J. Powder Metall.* **1988**, *24*, 59.
[46] D. C. Dunand, J. Teisen, in *Porous and Cellular Materials for Structural Applications (Eds: D. S. Schwartz, D. S. Shih, H. N. G. Wadley, A. G. Evans), MRS, Pittsburgh*, **1998, 231.**
[47] N. G. Davis, J. Teisen, C. Schuh, D. C. Dunand, *J. Mater. Res.* **2001**, *16*, 1508.
[48] R. Ricceri, P. Matteazzi, *Intern. J. Powder Metall.* **2003**, *39*, 53.
[49] R. L. Martin, R. J. Lederich, *Metal Powder Report* **1992**, 30.
[50] D. S. Schwartz, D. S. Shih, R. J. Lederich, R. L. Martin, D. A. Deuser, in *Porous and Cellular Materials for Structural Applications (Eds: D. S. Schwartz, D. S. Shih, A. G. Evans, H. N. G. Wadley), MRS, Pittsburgh*, **1998**, 225.
[51] D. M. Elzey, H. N. G. Wadley, *Metall. Mater. Trans. A* **1999**, *30*, 2689.
[52] D. T. Queheillalt, B. W. Choi, D. S. Schwartz, H. N. G. Wadley, *Metall. Mater. Trans. A* **2000**, *31*, 261.
[53] R. Vancheeswaran, D. T. Queheillalt, D. M. Elzey, H. N. G. Wadley, *Metall. Mater. Trans. A* **2001**, *32*, 1813.
[54] D. M. Elzey, H. N. G. Wadley, *Acta Mater.* **2001**, *49*, 849.
[55] G. W. Greenwood, R. H. Johnson, *Proc. Roy. Soc. Lond.* **1965**, *283A*, 403.
[56] D. C. Dunand, C. M. Bedell, *Acta Mater.* **1996**, *44*, 1063.
[57] M. Frary, C. Schuh, D. C. Dunand, *Metall. Mater. Trans. A* **2002**, *33*, 1669.
[58] C. Schuh, D. C. Dunand, *J. Mater. Res.* **2001**, *16*, 865.
[59] C. Schuh, D. C. Dunand, *Scripta Mater.* **2001**, *45*, 631.
[60] N. G. D. Murray, D. C. Dunand, *Acta Mater.* **2004**, *526*, 2269.
[61] N. G. D. Murray, D. C. Dunand, Acta Mater. **2004**, *52*, 2279.
[62] N. G. D. Murray, D. C. Dunand, *Composites Sci. Tech.* **2003**, *63*, 2311.
[63] H. Li, S. M. Oppenheimer, S. I. Stupp, D. C. Dunand, L. C. Brinson, *Mater. Trans.* in print.
[64] N. G. D. Murray, C. A. Schuh, D. C. Dunand, *Scripta Mater.* **2003**, *49*, 879.

